

Special
Collection

pH-Dependent Protonation of Surface Carboxylate Groups in PsbO Enables Local Buffering and Triggers Structural Changes

Lisa Gerland,^{*,[a, b]} Daniel Friedrich,^[a, b] Linus Hopf,^[a, b] Eavan J. Donovan,^[a] Arndt Wallmann,^[a] Natalja Erdmann,^[a] Anne Diehl,^[a] Martin Bommer,^[c] Krzysztof Buzar,^[d] Mohamed Ibrahim,^[e] Peter Schmieder,^[a] Holger Dobbek,^[e] Athina Zouni,^[e] Ana-Nicoleta Bondar,^[d] Holger Dau,^[f] and Hartmut Oschkinat^{*,[a, b]}

Photosystem II (PSII) catalyzes the splitting of water, releasing protons and dioxygen. Its highly conserved subunit PsbO extends from the oxygen-evolving center (OEC) into the thylakoid lumen and stabilizes the catalytic Mn₄CaO₅ cluster. The high degree of conservation of accessible negatively charged surface residues in PsbO suggests additional functions, as local pH buffer or by affecting the flow of protons. For this discussion, we provide an experimental basis, through the determination of pK_a values of water-accessible aspartate and glutamate side-chain carboxylate groups by means of NMR. Their distribution is strikingly uneven, with high pK_a values around 4.9 clustered on the luminal PsbO side and values below 3.5 on the side facing PSII. pH-dependent changes in backbone chemical shifts in the area of the lumen-exposed loops are observed, indicating conformational changes. In conclusion, we present a site-specific analysis of carboxylate group proton affinities in PsbO, providing a basis for further understanding of proton transport in photosynthesis.

most likely an irreversible inactivation of PSII caused (or initiated) by Ca²⁺ release. For these reasons, the photosynthetic organism will prevent a luminal pH as low as 4.6. A luminal pH above 5 is optimal for PSII function. In the thylakoid lumen, on the other hand, a pH close to 5 is needed for ensuring a trans-thylakoid pH gradient that suffices for driving ATP synthesis. A mechanism avoiding lower luminal pH values is energy-dependent quenching (qE), a component of the intensively studied non-photochemical quenching (NPQ),^[5–8] during which heat is generated instead of photochemical energy. The initiation of qE is directly coupled to the luminal pH and is the fastest component of NPQ.^[9,10]

Introduction

Photosynthesis involves a light-dependent primary reaction, effecting the splitting of water, and a light-independent secondary reaction, during which carbon dioxide is assimilated.^[1] The primary reaction is mediated by Photosystems I (PSI) and II (PSII), linked by a chain of redox-active molecules.

PSII, located in the thylakoid membranes of photosynthetically active cells, splits two water molecules into four protons, four electrons, and one dioxygen molecule at the oxygen-evolving center (OEC) containing a Mn₄CaO₅ cluster.^[2,3] Because high proton concentrations in the vicinity of the OEC are counterproductive in this process, continuous removal of protons is required. The O₂-formation step of PSII is indeed inhibited at low pH, with a half-inhibition pH of 4.6.^[4] At lower pH, there is

most likely an irreversible inactivation of PSII caused (or initiated) by Ca²⁺ release. For these reasons, the photosynthetic organism will prevent a luminal pH as low as 4.6. A luminal pH above 5 is optimal for PSII function. In the thylakoid lumen, on the other hand, a pH close to 5 is needed for ensuring a trans-thylakoid pH gradient that suffices for driving ATP synthesis. A mechanism avoiding lower luminal pH values is energy-dependent quenching (qE), a component of the intensively studied non-photochemical quenching (NPQ),^[5–8] during which heat is generated instead of photochemical energy. The initiation of qE is directly coupled to the luminal pH and is the fastest component of NPQ.^[9,10]

[a] L. Gerland, Dr. D. Friedrich, L. Hopf, E. J. Donovan, Dr. A. Wallmann, N. Erdmann, Dr. A. Diehl, Dr. P. Schmieder, Prof. H. Oschkinat
Leibniz-Forschungsinstitut für Molekulare Pharmakologie, Department of NMR-Supported Structural Biology
Robert-Rössle-Strasse 10, 13125 Berlin (Germany)
E-mail: gerland@fmp-berlin.de
oschkinat@fmp-berlin.de

[b] L. Gerland, Dr. D. Friedrich, L. Hopf, Prof. H. Oschkinat
Freie Universität Berlin, Department of Biology, Chemistry and Pharmacy
Thielallee 63, 14195 Berlin (Germany)

[c] Dr. M. Bommer
Max-Delbrück-Centrum für Molekulare Medizin
Robert-Rössle-Strasse 10, 13125 Berlin (Germany)

[d] K. Buzar, Prof. A.-N. Bondar
Freie Universität Berlin
Department of Physics, Theoretical Molecular Biophysics
Arnimallee 14, 14195 Berlin (Germany)

[e] Dr. M. Ibrahim, Prof. H. Dobbek, Prof. A. Zouni
Humboldt-Universität zu Berlin, Institute of Biology
Philippstrasse 13, 10099 Berlin (Germany)

[f] Prof. H. Dau
Freie Universität Berlin, Department of Physics, Biophysics and Photosynthesis
Arnimallee 14, 14195 Berlin (Germany)

Supporting information and the ORCID identification numbers for the authors of this article can be found under <https://doi.org/10.1002/cbic.201900739>.

© 2020 The Authors. Published by Wiley-VCH Verlag GmbH & Co. KGaA. This is an open access article under the terms of the Creative Commons Attribution License, which permits use, distribution and reproduction in any medium, provided the original work is properly cited.

This article is part of a Special Collection on the occasion of Horst Kessler's 80th birthday. To view the complete collection, visit our homepage.

It has been suggested that the evolutionarily conserved extrinsic PSII subunit PsbO, which is located at the luminal side of PSII (Figure 1 A), might provide a small buffering capacity^[11] or pathways for proton removal,^[12–14] or might act as a proton antenna,^[11] in addition to its established function in controlling the chloride and calcium concentrations at the OEC, thereby (and possibly also by other means) stabilizing the manganese complex.^[14–16] A pH buffer functionality of the PsbO carboxylate groups could transiently avoid acidification of the thylakoid lumen, for conditions of fluctuating light intensities (but not under continuous illumination), that easily and often occur in a natural habitat. This process might be relevant in a time segment of 5–20 s,^[17] which is a typical time regime for luminal

acidification after an increase in light intensity in an intact organism. The fast luminal acidification is directly coupled to a protective quenching of an excited antenna state (qE), followed by activation of slower protection mechanisms.^[5,6]

X-ray crystallography^[2,14] and computation^[13,18,19] suggested an extended proton network around the OEC, serving as starting point for proton transport pathways towards the thylakoid lumen. PsbO interacts with subunits D1 and D2 of PSII through the loops Asp158–Lys188 and Asp222–Ala228,^[20] and their residues Asp158, Asp222–Asp224, His228, and Glu229 are part of a putative proton exit pathway.^[12–14,18,21] The smallest distance between PsbO and the OEC is 17 Å, as measured in a PSII crystal structure (PDB ID: 3WU2^[22]). As shown in Figure 1, PsbO reaches out far into the luminal space. It exposes a considerable number of carboxylate groups on the surface of its β -barrel.^[12,18,20] These are largely solvent-accessible, show a surprisingly high degree of conservation^[20] (Figure S1), and might potentially affect proton flows from the OEC.^[11,12,15,18,20] Proton or water transport directly through the interior of the β -barrel is unlikely because it is blocked by bulky hydrophobic residues.^[23]

A tendency of PsbO to undergo pH-dependent structural changes was initially mentioned in conjunction with an observed hysteresis in acid–base titration experiments of isolated PsbO.^[24] Through a combination of molecular simulations and crystal structure analyses, it has been observed that upon deprotonation of the carboxylate dyad—Glu97(residue 90 in investigated construct), Asp102(95)—the Asp102 side chain moves away from Glu97 and Lys123(116).^[25] This happens at pH values between 6 and 10. These amino acid residues are at the interface between PsbO, PsbU, and CP43. Recent computations and analyses of crystal structures of PSII indicated that the interface between PsbO and PsbU hosts several hydrogen-bonded water molecules and an extensive network of water-mediated bridges between carboxylate groups; the energy barrier for proton transfer from Asp102(95) is high, and this could be interpreted as suggesting that a proton bound at this site could remain on the surface of the protein, at least transiently.^[26] To provide further experimental data relating to PsbO's potential role in proton management, we determined the pK_a values of aspartate and glutamate side-chain carboxylate groups on the surface of the PsbO barrel by NMR. For this purpose, we employed a soluble construct^[25] lacking the loops close to the OEC and studied the acidic residues directly situated on the barrel (Figure 1B). In detail, the PsbO- β construct used here and studied before by X-ray crystallography^[25] did not contain the N-terminal residues 1–15 or the residues in three loop regions (55–63, 149–192, and 220–231). The loop residues were omitted because they would not be structured in the isolated subunit lacking PSII interactions partners. All aspartate and glutamate residues remaining in the PsbO- β construct are on the outer surface of full-length PsbO within the PSII complex and solvent-accessible. In the following sections, we employ the numbering of full-length PsbO and indicate trimmed construct numbers in brackets.

Over the pH range of 2.0–7.0, the ¹³C chemical shifts of side-chain carboxylate groups can change strongly,^[27] depending

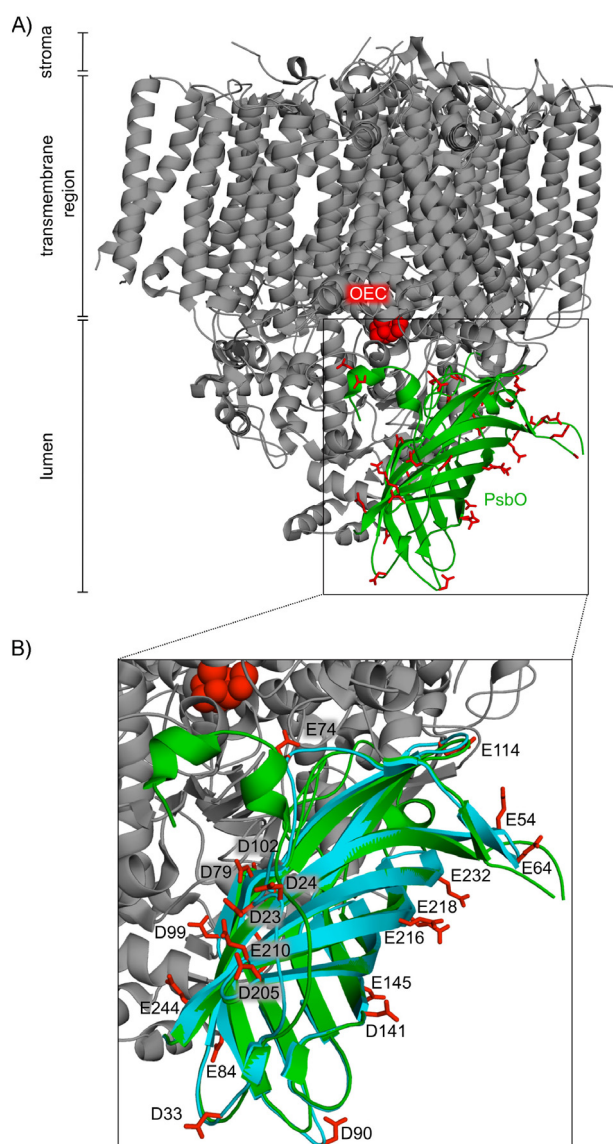


Figure 1. Location of PsbO in photosystem II monomer. A) The crystal structure of PSII of *Thermosynechococcus vulcanus* (PDB ID: 3WU2^[22]) shows the localization of PsbO (green). It is thought to contribute to proton transport from the OEC (depicted in red spheres) to the thylakoid lumen. PsbO features a number of surface aspartate and glutamate carboxylate groups^[11,12] (red). B) Overlay of full-length PsbO in green and the shorter PsbO- β in teal. Glutamate and aspartate residues of PsbO- β are depicted as sticks, and the residue numbers are consistent with the numbering of full-length PsbO.

on the formation or disruption of a hydrogen bond. This provides the basis for determining the pK_a values of such moieties through pH titrations and fitting the course of chemical shift changes to the Henderson–Hasselbalch equation^[28,29] (Figure S2). Our assignment of the side-chain carboxylate group signals of PsbO thus enabled the determination of 21 pK_a values in a residue-specific manner. As one striking result, we found a strong regional difference of pK_a values on the protein surface, suggesting an influence on charge distribution, local pH, buffering capacity, and proton flow.

Results

Determination of pK_a values of glutamate and aspartate carboxylate groups

We determined proton affinities of the glutamate and aspartate carboxylate groups by monitoring the chemical shifts of the $^{13}C_\gamma$ and $^{13}C_\delta$ atoms, respectively. This required the assignment of the $^{13}C_{\alpha}$, $^{13}C_{\beta}$, $^{13}C_\gamma$, $^{13}C_\delta$, ^{15}N , and $^1H^N$ resonances of PsbO- β , which was achieved to 98% completeness through triple-resonance experiments (Figures S3 and S4). To assign the chemical shifts of side-chain carbon atoms in glutamate and aspartate residues, we employed ^{13}C -detected, 3D CBCACO experiments.^[30] pH titrations were monitored by 2D CBCACO spectroscopy, yielding correlations involving $^{13}C_\gamma$ and $^{13}C_\delta$ chemical shifts of aspartate and glutamate, respectively (Figure 2A). We observed well-resolved crosspeaks, thus enabling precise interpretation of chemical shift changes of the carboxylate group carbons upon pH titration; see, for example, Asp141(134). The corresponding crosspeaks display pH changes in the range of 7.6 to 5.8 as indicated by the black arrow. Using this approach, we determined the pK_a values for a one-step proton-exchange mechanism, applying a nonlinear least-squares fit function. The titration curves of 21 aspartic and glutamic acid residues in PsbO- β are shown in Figure 2B and 2C, respectively. In most cases, the applied Henderson–Hasselbalch equation fits the experimental data reasonably well, such as in the cases of residues Asp23(23) and Asp141(134). However, the fit is less perfect for Glu210(161), Glu218(169), Glu232(176), and Asp205(156). The titration curves of these residues deviate in areas adjacent to the inflection points, thus indicating proton exchange involving additional sites: that is, two-step exchange mechanisms. Instructive examples are provided by the two clusters Asp23(23)/Glu210(161)/Asp205(156) and Glu216(167)/Glu218(169)/Glu232(176). In those clusters, protons are potentially shared through bifurcated hydrogen bonds (Figure 2D, left and right), so deviations of several data points from the fit function (Figure S2 in the Supporting Information) are observed. The corresponding crosspeaks of Asp79(72) (Figure 2B, red), Asp99(92) (Figure 2B, dark blue), and Asp102(95) (Figure 2B, violet) migrate during pH titration into a spectral region with heavy overlap of resonances, or vanish at certain pH values. For these reasons, some curves are incomplete and the pK_a value can therefore only be estimated as an upper or lower boundary.

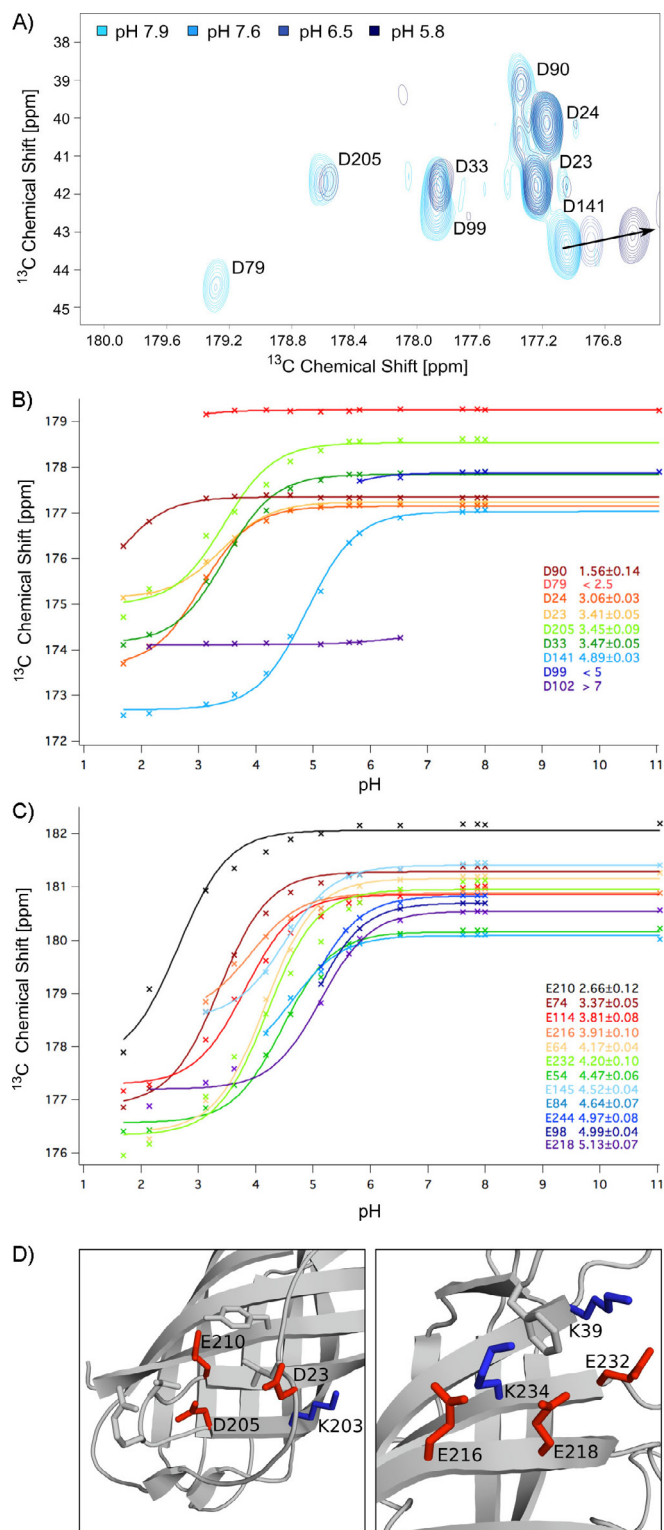


Figure 2. pH titration experiments and analysis. A) 2D CBCACO spectra at different pH values between pH 5.8 (dark blue) and pH 7.9 (light blue). The black arrow indicates the chemical shift changes of the Asp141 side-chain carboxylate group carbon with the pH shift. B) Observed titration curves of aspartic acid residues and the obtained pK_a values (95% confidence intervals are given as errors) are color-coded from low (red) to high (blue) values. C) Titration curves of glutamic acid residues with pK_a values and 95% confidence intervals are color-coded from low (black) to high (purple). D) The side chain conformations of residues displaying side-chain carboxylate group carbon resonances that do not shift in close agreement with the Henderson–Hasselbalch equation are shown in the crystal structure of PsbO- β .^[25]

Most of the glutamic acid pK_a values cluster around the standard value of 4.25 for glutamic acid in solution,^[31] with the two exceptions of Glu74(67) ($pK_a = 3.37 \pm 0.05$) and Glu210(161) ($pK_a = 2.66 \pm 0.12$) being more acidic.

The variance of the pK_a values of aspartic acid residues was strikingly high, with four of them differing strongly from the standard value of 3.67 ± 0.04 ^[31] for aspartic acid in solution. Asp102(95) ($pK_a > 7$) and Asp141(134) ($pK_a = 4.89 \pm 0.03$) exhibit very high pK_a values, whereas Asp90(83) ($pK_a = 1.56 \pm 0.14$) is the most acidic. To our surprise, this amino acid is part of a flexible loop, which implies a higher pK_a for this residue. The low pK_a value of Asp79(72) ($pK_a < 2.5$) might be explained by a neighboring disulfide bridge, which might stabilize the negative charge, leading to a lower pK_a value.

In summary, we determined the pK_a values for 21 aspartate and glutamate carboxylate groups on the PsbO- β surface. All are solvent-accessible in full-length PsbO within the PSII complex. The pK_a of Glu97(90) is missing because crosspeaks involving the C_β could not be assigned.

Calculation of pK_a values with ProPKa 3.0^[32] (for details see the Supporting Information, in particular Figure S5) showed a reasonable agreement between predicted and measured pK_a values (Table 1), with the greatest difference for Glu98(91) ($\Delta = 1.03$) followed by Glu210(161) ($\Delta = 0.97$). As expected, the calculated values for residues with extreme pK_a values diverged more strongly from the measured data than those with values closer to the average pK_a .

Asp residue no.	pK_a value	Glu residue no.	pK_a value
23	3.41 ± 0.05	54	4.47 ± 0.06
24	3.06 ± 0.03	64	4.17 ± 0.04
33	3.47 ± 0.05	74	3.37 ± 0.05
79	< 2.5	84	4.64 ± 0.07
90	1.56 ± 0.14	98	4.99 ± 0.04
99	< 5	114	3.81 ± 0.08
102	> 7	145	4.52 ± 0.04
141	4.89 ± 0.03	210	2.66 ± 0.12
205	3.45 ± 0.09	216	3.91 ± 0.10
		218	5.13 ± 0.07
		232	4.20 ± 0.10
		244	4.97 ± 0.08

Chemical shift perturbations (CSPs) of PsbO backbone amide groups

In order to investigate whether pH changes over the range of 2–8 induce conformational rearrangements, and to establish whether or not the protein remains folded towards low pH, the titration was also monitored by 2D 1H , ^{15}N correlation spectroscopy. We observed strong chemical shift changes for several residues, together with negligible changes for the larger fraction of 2D crosspeaks (Figures 3A, B and S6). Figure 3A displays the pH-dependent CSPs that we were able to analyze. In Figure 3B the side chains of residues exhibiting the strongest shifts are shown within the PsbO- β X-ray structure, with indications of strength ranging from strong (> 0.2) in dark blue to

medium ($0.17 < CSP < 0.2$) in light blue. Small changes below 0.17 are not displayed because we consider them less significant. On the whole, the residues showing the largest changes are clustered towards the loops on the luminal side of the barrel, with Thr25(25), Thr208(159), and Ala246(191) showing the largest effects. Interestingly, the cyano loop that mediates contacts between PSII dimers^[33] is surrounded by residues with amide group signals that are pH-sensitive; hence it is not excluded that conformational changes modulate the dimer contacts. We noticed only intermediate CSP values for residues of the proposed structural switch region: Glu98(91) and Asp99(92). Another residue of this switch region—Asp102(95)—shows an unexpectedly small CSP. Interestingly, we were only able to assign peaks for Asp102(95) from pH 3.1 to 6.5. The possibility of a moderate chemical shift change in this range agrees with Asp102(95) altering its position in the carboxylate dyad after deprotonation between pH 6 and 10.

Discussion

The PSII activity determines the luminal pH in thylakoids. Under optimal light conditions this can drop to a value of 5. Because a lower pH would strongly reduce the stability of PSII and inactivate the manganese complex, the activity of the photosystem needs to be regulated. The half-inhibition point of the water oxidation reaction at PSII is already reached at pH 4.6.^[4] pH values below this point will lead to irreversible inactivation, believed to be controlled by calcium release.^[34] At pH values above 5, on the other hand, the transmembrane proton gradient (ΔpH) of the proton motive force (PMF) would be reduced and possibly too small to provide enough protons for ATP synthesis. This turns luminal pH control into an important task for photoactive plants and bacteria, and, due to its exposed position, PsbO might crucially contribute to this process. However, not all of the PsbO surface is solvent-exposed (Figure 1A and B). Apart from contacts with various PSII subunits, PsbO–PsbO contacts exist in the native-like PSII X-ray structure,^[33] formed by the cyano loops of two PsbO molecules (Figures 4A and S7). Of the loop residues, Thr138(131) and Ser139(132) form hydrogen bonds to one another^[33] (Figure S7). The reported arrangement of dimers in a row is considered to be similar to the situation in native thylakoid membranes of spinach and pea.^[35]

Prior to the interpretation of the pK_a values, and given a dimer arrangement of PSII, it is instructive to have a look at the electrostatic properties of the PsbO surface at pH 7. These are shown in Figure 4A for the dimer as it exists in the crystal structure (PDB ID: 4PJ0^[33]): as illustrated in the top panel, the contact areas between the two PsbO molecules are small, and a band of negative potential made up by residues Asp23(23), Asp24(24), Glu79(72), Glu205(156), and Glu210(161) is present on the other side, nearly forming a ring around the dimer. A second band of negative potential covers the area including Glu97(90), Glu98(91), Asp99(92), and Asp102(95). Apart from Asp99(92), all negatively charged residues are exposed to the lumen and are not involved in interactions with other PSII proteins (Figure S8). The pK_a values represent a quantification of

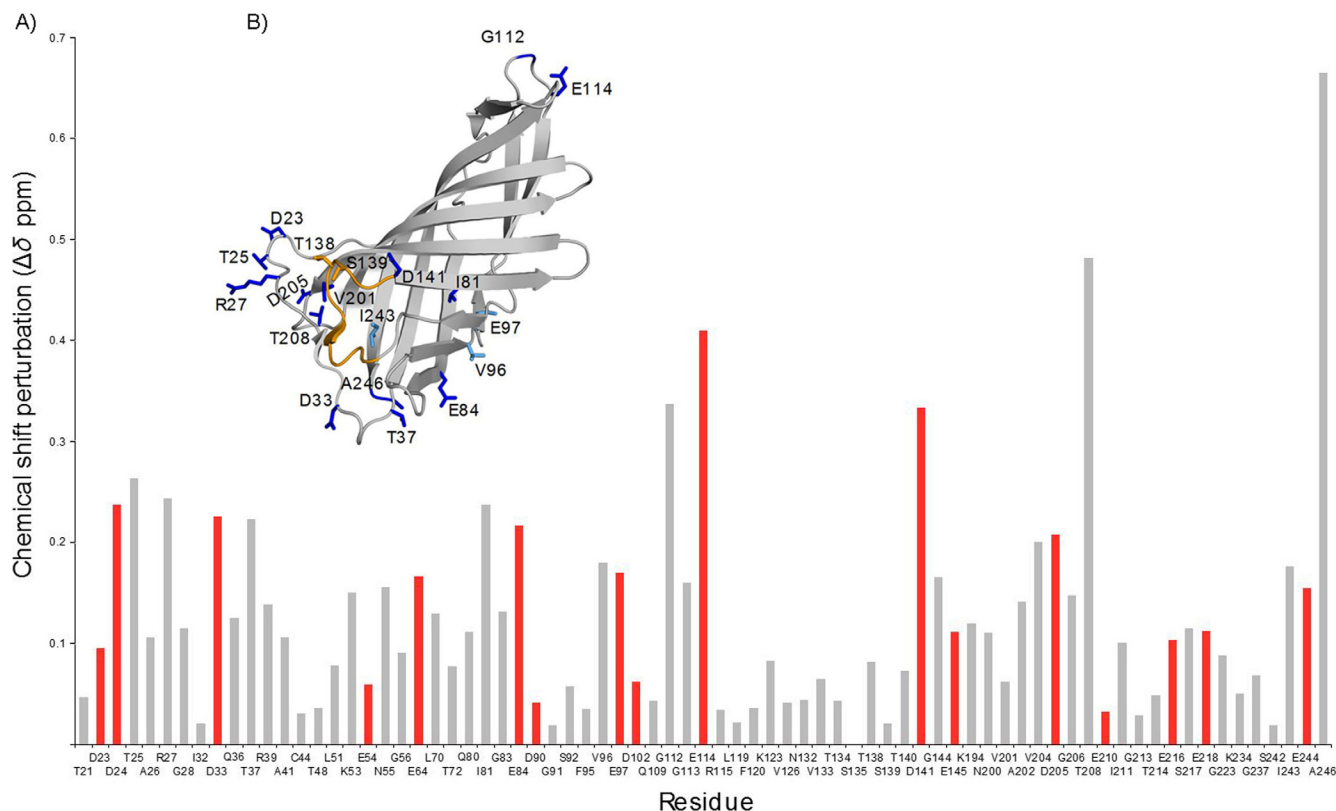


Figure 3. CSP measurements by 2D $^1\text{H},^{15}\text{N}$ correlation spectroscopy to monitor conformation changes in PsbO- β . A) $^{15}\text{N},^1\text{H}$ CSPs of all residues that could be evaluated (acidic residues are highlighted in red, CSPs were calculated by a formula provided in the Experimental Section. The residues N55, G56, and G223 were inserted as loop replacements during trimming of the long construct and are not part of the original PsbO sequence. B) Residues with strongest CSPs plotted on the crystal structure of PsbO- β (PDB ID: 5G39^[25]), color-coded from high (≥ 0.2 , dark blue) to intermediate values ($0.17 \leq \text{CSP} \leq 0.2$, light blue). Residues with small CSPs (< 0.17) are not displayed; amino acids that are part of the cyano loop are shown in orange and those involved in PSII dimer contacts as sticks.

pH effects on the charge of the protein. At first, it is surprising that the obtained values span a comparably wide region of the pH scale (Figure 4B), ranging from 1.56 to 5.13 [potentially even higher for Asp99(92) and Asp102(95)], independent of the specific amino acid (Glu or Asp). For a detailed analysis, we show the side chains of the negatively charged residues with their pK_a values and color-coded in the crystal structure of PsbO- β (Figure 4C, D). We observe a specific pK_a distribution with lower values clustering on the lumen-exposed side of PsbO, whereas the area closer to PSII harbors residues with higher pK_a values, as revealed by analyzing the pK_a distribution on the PsbO- β surface in complex with PSII (PDB ID: 2AXT^[36], Figure 4D). A special role relating to buffering in the pH range between 4 and 7 is played by the carboxylate groups.^[20] Of the 22 side-chain carboxylate groups, eight in our short PsbO- β construct show pK_a values in the functionally relevant range from 4.3 to 5.1. Those residues are largely located at the side of PsbO facing the lumen (Figure 4C, D).

Given the number of PsbO carboxylate groups relative to the extent of luminal space and protein density, PsbO's buffering capacity in this range is limited, yet those residues are in a suitable area: that is, not far from the potential proton release site (Figure 4D). This might help in bypassing the first seconds of luminal acidification before downregulation of PSII activity

through NPQ mechanisms takes over. The surprisingly wide distribution of pK_a values might affect the characteristics of PsbO's overall buffering capabilities. On generating the mean value of all curves, we find an elongated, less steep transition to the protonated state of the protein (Figure S9), with an inflection point around 4.1. Intriguingly, the pK_a values of the "negative band" involving residues Asp23(23), Asp24(24), Glu79(72), Glu205(156), and Glu210(161) are well or just below 4.0, which means they always remain deprotonated at any state of PSII activity. In contrast, the band of residues made up by Glu64, Glu84, Glu97, Glu98, Asp102, Asp141, Glu145, Glu218, Glu232, and Glu244 (Figure 4C, D) become protonated over a pH range between 4.0 and 5.0. Because the low- pK_a patch remains deprotonated down to a pH of 4.0, PsbO thus experiences a change in distribution of surface charges that might be the basis for a pH-dependent switch.

In this context, it is interesting that pH-dependent changes in the backbone chemical shifts indicative of structural changes are clustered at the luminal side of PsbO comprising the low- pK_a patch (Figure 3A, B). In particular, residues in the loops exposed to the lumen and in the corresponding ends of the β -strands are affected, as well as a stretch involving Glu84(77), Val96(89), and Glu97(90). The structural changes extend towards the PsbU interaction area, so it is conceivable

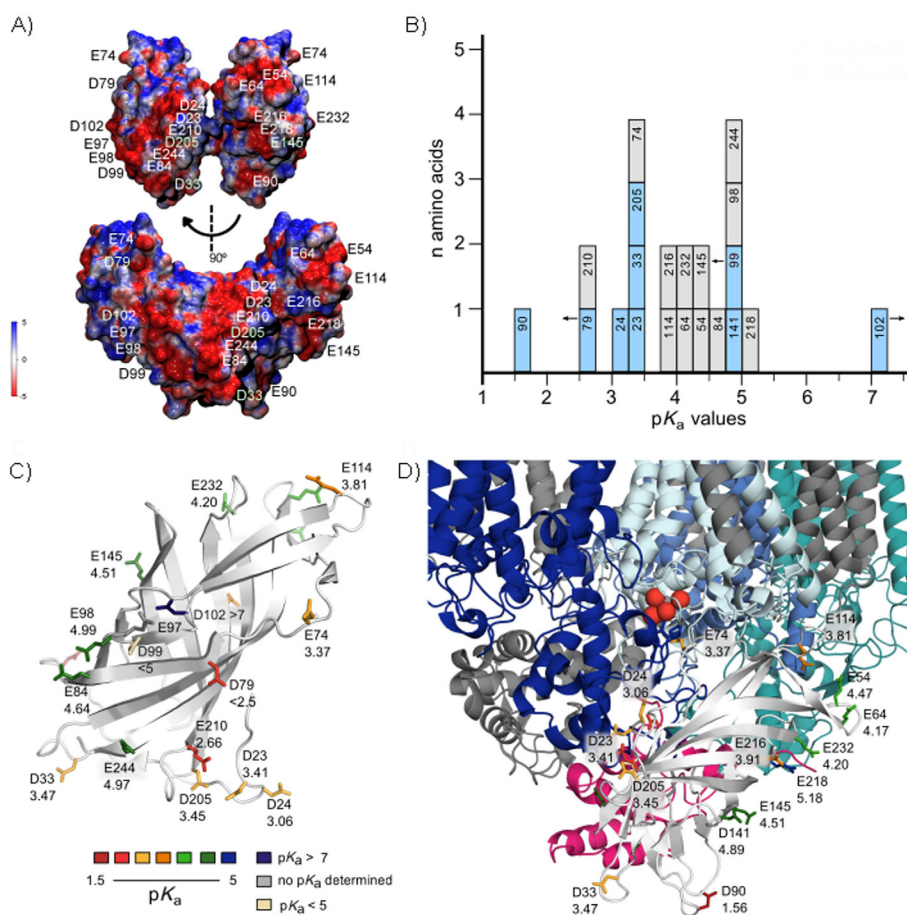


Figure 4. Distribution of pK_a values on the surface of PsbO- β : interpretation in the context of PSII. A) Electrostatic potentials of amino acid residues plotted onto a surface created with van der Waals distances of PsbO- β . B) Histogram demonstrating the pK_a distribution of carboxylic acid residues (pK_a axis divided into units of 0.25). Glutamic acid residues are shown in blue and aspartic acid residues in grey. The numbers indicate the amino acid position in full-length PsbO. pK_a values of residues shown with an arrow could not be determined accurately; the arrows indicate that these values are below or above the given pK_a . C) The crystal structure of the PsbO- β construct of *T. elongatus* (PDB ID: 5G39^[25]) shown in light gray, with glutamate and aspartate residues depicted as sticks, color-coded according to their pK_a values. The residue numbers follow the nomenclature of full-length PsbO. D) Close-up of PsbO- β (PDB ID: 5G38^[25]) in complex with PSII (PDB ID: 2AXT^[36]) and the associated proteins D1 (pale blue), D2 (blue), CP43 (dark blue), CP47 (turquoise), and PsbU (pink). The atoms of the OEC are shown as red spheres.

that they modulate the interaction between PsbO and PSII. A structural coupling between PsbO and OEC function has been concluded from FTIR difference spectroscopy.^[15,37] Our data preclude pH-induced opening of the barrel structure. The majority of residues in the upper part of the β -barrel structure (Figure 3B) feature small CSPs (<0.17) over a range from pH 3.1 to 7.9. Most of the protein thus shows high rigidity in our experiments, even at pH values below 4.

Conclusions

We have determined, or estimated, 21 out of 22 pK_a values associated with aspartic acid and glutamic acid residues in PsbO- β . Their uneven distribution on the luminal and PSII-facing sides of the β -barrel leads to an altered charge distribution at pH values between 3.5 and 5 within the thylakoids. This correlates with additional structural changes in PsbO as monitored by chemical shift changes of backbone amide groups. Overall, the induced structural changes might modify contacts between PsbO and other PSII proteins, as well as help to modu-

late the activity of the photosystem, thereby complementing the qE mechanism by a second route of pH-induced downregulation of PSII activity. We note that upon protonation of crucial PsbO residues any related structural changes are likely to proceed on a very fast timescale, but because the luminal acidification (and thus PsbO side-chain protonation) requires several seconds, the structural changes will become effective only on the seconds timescale. The rate-determining step in the process is thus not these pH-induced structural changes, but the acidification.

Further experiments based on our findings—for example, studying surface water molecules located at the interface between protein and surrounding fluid and that might play an important role in proton management—might prove informative. Room-temperature neutron diffraction experiments for determining the locations of water molecules at the PsbO surface were performed by Bommer et al.^[38] Further work relating to surface water molecules could complement these studies of PsbO's role in PSII. Generating pH-dependent PSII structures with X-ray free electron lasers might elucidate the structural

regulation of PsbO and other extrinsic subunits, as well as the interactions of PSII and PsbO with intrinsic subunits such as D1, D2, CP47, and CP43.

Experimental Section

Protein expression, purification, and sample preparation: Details of the design and cloning of the *Thermosynechococcus elongatus* β -barrel PsbO (PsbO- β) construct are described in Bommer et al.^[25] The PsbO- β construct in PET28a was transformed in *Escherichia coli* BL21(DE3) cells by following a standard heat shock protocol. Cells were plated and grown on lysogeny broth (LB) agar, with kanamycin (40 $\mu\text{g mL}^{-1}$) at 37 °C overnight. Transformants were used to inoculate a LB preculture with kanamycin (25 °C, 180 rpm overnight). Cells were centrifuged for 10 min at 2000 g and RT, and the pellet was washed and resuspended in ^{13}C and ^{15}N M9 medium (2 L). Cells were grown at 37 °C and 170 rpm, reaching an OD of 0.4, at which expression was induced with isopropyl β -D-thiogalactopyranoside (IPTG, 1 mM), and cells were harvested after 5 h at 37 °C and 170 rpm.

Cell pellets (2 g) were resuspended in ice-cold 2-morpholin-4-yl-ethanesulfonic acid (MES) buffer (pH 6.6, 30 mM, 30 mL) with MgCl_2 (2 mM). HS nuclease (250 units μL^{-1} Mobitec, Germany, 15 μL) was added, and cells were disrupted by using a microfluidizer (15000 psi). Cell debris was spun down (30 min, 48000 g, 25 °C), and the supernatant was incubated for 4 h at RT to digest the DNA effectively. Because the source of the PsbO is a thermophilic cyanobacterium we applied a purification protocol with an incubation step at 75 °C for 30 min. Most of the *E. coli* proteins denatured, with PsbO remaining in the supernatant after centrifugation (20 min, 48000 g, 8 °C).

The supernatant was concentrated with Amicon Ultra 4 mL filters (3k MWCO) to 1.2 mL and added through a 0.45 μm filter. Size-exclusion chromatography was performed (120 mL Superdex 75) with MES (pH 6.6, 30 mM). Fractions containing PsbO- β were combined and concentrated 50-fold to a final concentration of 35 mg mL^{-1} by using an Amicon Ultra 4 mL filter (3k MWCO).

For NMR titration measurements, the PsbO- β sample concentration was adjusted to between 9 and 14 mg mL^{-1} . To adjust the pH, samples were dialyzed overnight. A sodium phosphate buffer (20 mM) was used for a pH range between 5 and 8; for lower pH values phosphoric acid (20%) was added, whereas for higher pH values NaOH (1 M) was used. All samples contained D_2O (10%); the pH and protein concentration were measured after the addition of D_2O and before starting the NMR measurements.

NMR spectroscopy: Spectra were recorded with AV-III-600 spectrometers and cryogenically cooled probes (Bruker Biospin, Karlsruhe, Germany) at 300 K. The backbone was assigned by using HNC0, HNCACB, HN(CO)CACB, and HN(COCACB)CG 3D transverse relaxation-optimized spectra (TROSY). The HNC0 was recorded with an acquisition time of 51 ms in F_3 (^1H), 15.9 ms in F_2 (^{15}N), and 19.2 ms in F_1 (^{13}C), four scans, $512 \times 48 \times 48$ complex points, and spectral widths of 10000 (^1H), 3012 (^{15}N), and 2500 Hz (^{13}C) in the direct and indirect dimensions. HNCACB, HN(CO)CACB, and HN(COCACB)CG were recorded with acquisition times of 51 ms in F_3 (^1H), 16.6 ms in F_2 (^{15}N), and 5.5 ms in F_1 (^{13}C), eight scans, $512 \times 50 \times 55$ complex points, and spectral widths of 10000 (^1H), 3012 (^{15}N), and 10000 Hz (^{13}C) in the direct and indirect dimensions. ^{15}N , ^1H HSQC spectra were recorded with acquisition times of 51 ms in F_2 (^1H) and 85 ms in F_1 (^{15}N), eight scans, 512×256 complex points, and spectral widths of 10000 and 3012 Hz in the direct and indirect di-

mension. The side-chain assignment was performed with the aid of 3D CBCACO spectra. They were recorded with acquisition times of 51 ms in F_3 (^{13}C), 9.1 ms in F_2 (^{13}C), and 7 ms in F_1 (^{13}C), four scans, $512 \times 64 \times 70$ complex points, and spectral widths of 10000 (^1H), 7042 (^{15}N), and 10000 Hz (^{13}C) in the direct and indirect dimensions. 2D CBCACO titration spectra were recorded for 24 h with acquisition times of 51 ms in F_2 (^{13}C) and 6.4 ms in F_1 (^{13}C), 220 scans, 512×64 complex points, and spectral widths of 10000 Hz in the direct and indirect dimensions. Assignment spectra were recorded with triply labeled protein (^2H , ^{13}C , ^{15}N) whereas for the titration spectra and HSQC $^{13}\text{C}/^{15}\text{N}$ -labeled PsbO was used. All spectra were processed by using Topspin 3.2 and the assignment was performed with CCPNmr Analysis 2.4.

Calculation of CSP data: CSPs were calculated by use of the following formula: [Eq. (1)]

$$\text{CSP} = \sqrt{[\Delta\delta(\text{ppm})^1\text{H}]^2 + [0.156 \times \Delta\delta(\text{ppm})^{15}\text{N}]^2} \quad (1)$$

Calculations are based on pH-dependent shift differences [$\Delta\delta(\text{ppm})$] observed in 2D ^{15}N , ^1H HSQC spectra. We chose a pH range between 3.1 and 7.9 as standard for each residue if not stated otherwise. The data can be found in the Supporting Information.

Constructing a model of PsbO–PsbO interactions in the PSII dimer of dimers: Experiments have indicated that dimers of PSII can dimerize to tetramers,^[33,39] and that in such dimers-of-dimers complexes, PsbO proteins mediate direct hydrogen bonds between the PSII dimers.^[33] We thus used the crystal structure PDB ID: 4PJ0 of the PSII dimer^[40] and the crystal structure PDB ID: 5G38 of PsbO- β ^[20] to generate a structural model of the PsbO-mediated interactions between PSII dimers.

In the first step we used the transformation matrix reported with the crystal structure of the PSII dimer^[40] to generate a PSII dimer of dimers with PyMOL^[41] and we extracted the coordinates of the two PsbO copies that are in direct contact. In the second step we used visual molecular dynamics (VMD^[42]) to overlap the structure of PsbO- β with each of these two PsbO proteins. The overlap between PsbO- β and full-length PsbO was based on sequence analyses with ClustalW^[43] and on the findings of del Val et al.^[20]

The electrostatic potential for PsbO- β was calculated by using the PDB2PQR tool via the web interface^[39] to assign partial atomic charges from the CHARMM force field (Chemistry at Harvard Molecular Mechanics,^[40] and Adaptive Poisson–Boltzmann Solver (APBS)^[41] in VMD.

Acknowledgements

We acknowledge financial support by the German Research Foundation (DFG) provided to the Collaborative Research Center SFB 1078 (projects A4 to H. Dau, A5 to A.Z. and H.D., B1 to H.O., C4 to A.-N.B.), A.-N.B. also acknowledges financial support from the Excellence Initiative of the German Federal and State Governments provided by the Freie Universität Berlin. D.F. received support from the Human Frontier Science Program (HFSP, LT000022/2019-L) and is a non-stipendiary Fellow of the European Molecular Biology Organization (EMBO, ALTF 35–2019).

Conflict of Interest

The authors declare no conflict of interest.

Keywords: NMR spectroscopy · pH titration · photosystem II · pK_a values · protonation

- [1] J. Barber, *Philos. Trans. R. Soc. London Ser. B* **2008**, *363*, 2665–2674.
- [2] J. Kern, R. Chatterjee, I. D. Young, F. D. Fuller, L. Lassalle, M. Ibrahim, S. Gul, T. Fransson, A. S. Brewster, R. Alonso-Mori, et al., *Nature* **2018**, *563*, 421–425.
- [3] M. Suga, F. Akita, M. Sugahara, M. Kubo, Y. Nakajima, T. Nakane, K. Yamashita, Y. Umena, M. Nakabayashi, T. Yamane, et al., *Nature* **2017**, *543*, 131–135.
- [4] I. Zaharieva, J. M. Wichmann, H. Dau, *J. Biol. Chem.* **2011**, *286*, 18222–18228.
- [5] P. Müller, X. P. Li, K. K. Niyogi, *Plant Physiol.* **2001**, *125*, 1558–1566.
- [6] A. V. Ruban, *Plant Physiol.* **2016**, *170*, 1903–1916.
- [7] A. Kanazawa, E. Ostendorf, K. Kohzuma, D. Hoh, D. D. Strand, M. Sato-Cruz, L. Savage, J. A. Cruz, N. Fisher, J. E. Froehlich, D. M. Kramer, *Front. Plant Sci.* **2017**, *8*, 1–12.
- [8] U. Armbruster, V. Correa Galvis, H. H. Kunz, D. D. Strand, *Curr. Opin. Plant Biol.* **2017**, *37*, 56–62.
- [9] E. Kress, P. Jahns, *Front. Plant Sci.* **2017**, *8*, 1–17.
- [10] A. Jajoo, M. Szabó, O. Zsiros, G. Garab, *Biochim. Biophys. Acta Bioenerg.* **2012**, *1817*, 1388–1391.
- [11] T. Shutova, V. V. Klimov, B. Andersson, G. Samuelsson, *Biochim. Biophys. Acta Bioenerg.* **2007**, *1767*, 434–440.
- [12] S. Lorch, S. Capponi, F. Pieront, A. N. Bondar, *J. Phys. Chem. B* **2015**, *119*, 12172–12181.
- [13] F. Guerra, M. Siemers, C. Mielack, A. N. Bondar, *J. Phys. Chem. B* **2018**, *122*, 4625–4641.
- [14] H. Ishikita, W. Saenger, B. Loll, J. Biesiadka, E. W. Knapp, *Biochemistry* **2006**, *45*, 2063–2071.
- [15] K. Ifuku, T. Noguchi, *Front. Plant Sci.* **2016**, *7*, 84.
- [16] T. M. Bricker, J. L. Roose, R. D. Fagerlund, L. K. Frankel, J. J. Eaton-Rye, *Biochim. Biophys. Acta Bioenerg.* **2012**, *1817*, 121–142.
- [17] H. Dau, *J. Photochem. Photobiol. B* **1994**, *26*, 3–27.
- [18] A. N. Bondar, H. Dau, *Biochim. Biophys. Acta Bioenerg.* **2012**, *1817*, 1177–1190.
- [19] D. Kaur, X. Cai, U. Khaniya, Y. Zhang, J. Mao, M. Mandal, M. R. Gunner, *Inorganics* **2019**, *7*, 14.
- [20] C. del Val, A.-N. Bondar, *Biochim. Biophys. Acta Bioenerg.* **2017**, *1858*, 432–441.
- [21] J. Barber, K. Ferreira, K. Maghlaoui, S. Iwata, *Phys. Chem. Chem. Phys.* **2004**, *6*, 4737–4742.
- [22] Y. Umena, K. Kawakami, J. R. Shen, N. Kamiya, *Nature* **2011**, *473*, 55–60.
- [23] J. De Las Rivas, J. Barber, *Photosynth. Res.* **2004**, *81*, 329–343.
- [24] T. Shutova, K. D. Irrgang, V. Shubin, V. V. Klimov, G. Renger, *Biochemistry* **1997**, *36*, 6350–6358.
- [25] M. Bommer, A. N. Bondar, A. Zouni, H. Dobbek, H. Dau, *Biochemistry* **2016**, *55*, 4626–4635.
- [26] L. Kemmler, M. Ibrahim, H. Dobbek, A. Zouni, A.-N. Bondar, *Phys. Chem. Chem. Phys.* **2019**, *21*, 25449–25466.
- [27] M. Tollinger, J. D. Forman-Kay, L. E. Kay, *J. Am. Chem. Soc.* **2002**, *124*, 5714–5717.
- [28] D. F. K. Julie, G. M. Clore, M. G. Angela, *Biochemistry* **1992**, *31*, 3442–3452.
- [29] E. Bombarda, G. M. Ullmann, *J. Phys. Chem. B* **2010**, *114*, 1994–2003.
- [30] W. Bermel, I. Bertini, I. C. Felli, M. Piccioli, R. Pierattelli, *Prog. Nucl. Magn. Reson. Spectrosc.* **2006**, *48*, 25–45.
- [31] R. L. Thurlkill, G. R. Grimsley, J. M. Scholtz, C. N. Pace, *Protein Sci.* **2006**, *15*, 1214–1218.
- [32] M. H. M. Olsson, C. R. Søndergaard, M. Rostkowski, J. H. Jensen, *J. Chem. Theory Comput.* **2011**, *7*, 525–537.
- [33] J. Hellmich, M. Bommer, A. Burkhardt, M. Ibrahim, J. Kern, A. Meents, F. Müh, H. Dobbek, A. Zouni, *Structure* **2014**, *22*, 1607–1615.
- [34] A. Krieger, E. Weis, *Photosynth. Res.* **1993**, *37*, 117–130.
- [35] B. Daum, D. Nicastro, J. Austin, J. R. McIntosh, W. Kühlbrandt, *Plant Cell* **2010**, *22*, 1299–1312.
- [36] B. Loll, J. Kern, W. Saenger, A. Zouni, J. Biesiadka, *Nature* **2005**, *438*, 1040–1044.
- [37] A. R. Offenbacher, B. C. Polander, B. A. Barry, *J. Biol. Chem.* **2013**, *288*, 29056–29068.
- [38] M. Bommer, L. Coates, H. Dau, A. Zouni, H. Dobbek, *Acta Crystallogr. Sect. F Biol. Commun.* **2017**, *73*, 525–531.
- [39] T. J. Dolinsky, J. E. Nielsen, J. A. McCammon, N. A. Baker, *Nucleic Acids Res.* **2004**, *32*, W665–W667.
- [40] A. D. MacKerell, Jr., D. Bashford, M. Bellott, R. L. Dunbrack, J. D. Evanseck, M. J. Field, S. Fischer, J. Gao, H. Guo, S. Ha, et al., *J. Phys. Chem. B* **1998**, *102*, 3586–3616.
- [41] N. A. Baker, D. Sept, S. Joseph, M. J. Holst, J. A. McCammon, *Proc. Natl. Acad. Sci. USA* **2001**, *98*, 10037–10041.
- [42] W. Humphrey, A. Dalke, K. Schulten, *J. Mol. Graph.* **1996**, *14*, 33–38.
- [43] F. Madeira, Y. m. Park, J. Lee, N. Buso, T. Gur, N. Madhusoodanan, P. Basutkar, A. R. N. Tivey, S. C. Potter, R. D. Finn, R. Lopez, *Nucleic Acids Res.* **2019**, *47*, W636–W641.

Manuscript received: December 9, 2019

Accepted manuscript online: January 12, 2020

Version of record online: March 5, 2020